Science Translational Medicine
AAAS

www.sciencetranslationalmedicine.org/cgi/content/full/9/392/eaal3447/DC1

Supplementary Materials for

Neurokinin 1 receptor signaling in endosomes mediates sustained nociception and is a viable therapeutic target for prolonged pain relief

Dane D. Jensen, TinaMarie Lieu, Michelle L. Halls, Nicholas A. Veldhuis, Wendy L. Imlach, Quynh N. Mai, Daniel P. Poole, Tim Quach, Luigi Aurelio, Joshua Conner, Carmen Klein Herenbrink, Nicholas Barlow, Jamie S. Simpson, Martin J. Scanlon, Bimbil Graham, Adam McCluskey, Phillip J. Robinson, Virginie Escriou, Romina Nassini, Serena Materazzi, Pierangelo Geppetti, Gareth A. Hicks, Macdonald J. Christie, Christopher J. H. Porter,* Meritxell Canals,* Nigel W. Bunnett*

*Corresponding author. Email: nb2733@cumc.columbia.edu (N.W.B.); chris.porter@monash.edu (C.J.H.P.); meri.canals@monash.edu (M.C.)

Published 31 May 2017, *Sci. Transl. Med.* **9**, eaal3447 (2017)
DOI: 10.1126/scitranslmed.aal3447

The PDF file includes:

Other Supplementary Material for this manuscript includes the following:
(available at www.sciencetranslationalmedicine.org/cgi/content/full/9/392/eaal3447/DC1)

Movie S1 (.mp4 format). Three-dimensional projections of NK_1R-IR in neurons in spinal cord slices incubated with Dy4 inact and vehicle.
Movie S2 (.mp4 format). Three-dimensional projections of NK_1R-IR in neurons in spinal cord slices incubated with Dy4 inact and SP.
Movie S3 (.mp4 format). Three-dimensional projections of NK_1R-IR in neurons in spinal cord slices incubated with Dy4 and vehicle.
Movie S4 (.mp4 format). Three-dimensional projections of NK_1R-IR in neurons in spinal cord slices incubated with Dy4 and SP.
Movie S5 (.mp4 format). Three-dimensional projections of NK_1R-IR in neurons in spinal cord 10 min after intraplantar injection of vehicle.
Movie S6 (.mp4 format). Three-dimensional projections of NK_1R-IR in neurons in spinal cord 10 min after intraplantar injection of capsaicin.
Movie S7 (.mp4 format). Three-dimensional projections of NK_1R-IR in neurons in spinal cord 10 min after intraplantar injection of capsaicin, with Dy4 injected before capsaicin.
Movie S8 (.mp4 format). Three-dimensional projections of NK_1R-IR in neurons in spinal cord 10 min after intraplantar injection of capsaicin, with Dy4 inact injected before capsaicin.
Movie S9 (.mp4 format). Three-dimensional projections of NK_1R-IR in neurons in spinal cord 10 min after intraplantar injection of capsaicin, with PS2 injected before capsaicin.
Movie S10 (.mp4 format). Three-dimensional projections of NK_1R-IR in neurons in spinal cord 10 min after intraplantar injection of capsaicin, with PS2 inact injected before capsaicin.
Movie S11 (.mp4 format). Plasma membrane incorporation and endocytosis of Cy5-cholestanol by HEK293 cells.
Movie S12 (.mp4 format). Lack of uptake of Cy5–ethyl ester by HEK293 cells.
Movie S13 (.mp4 format). Time lapse images showing FRET between SNAP-549-NK_1R and Cy5-Chol.
Movie S14 (.mp4 format). Animation showing SP-induced assembly of endosomal signaling platform for pain transmission.

Materials and Methods

Animals. Institutional Animal Care and Use Committees approved all studies. Rats (Sprague-Dawley, males, 3-8 weeks) and mice (C57BL/6, males, 6-10 weeks) were from the Monash Animal Research Platform, the Animal Resources Centre, Western Australia, and Harlan Laboratories. Animals were maintained in a temperature-controlled environment with a 12 h light/dark cycle and free access to food and water. Animals were sacrificed by inhalation of isoflurane or carbon dioxide, or with sodium pentobartitone (200 mg/kg, i.p.), followed by bilateral thoracotomy or decapitation. Animals were randomized for treatments, and no animals were excluded from studies.

Tripartite probes. Cyanine 5, spantide I, and L-733,060 were conjugated to cholestanol or aspartate ethyl ester via a flexible PEG linker by standard Fmoc solid-phase peptide synthesis (SPPS) on Fmoc-PAL-PEG-PS resin (Life Technologies, 0.17 mmol/g resin loading) (fig. S9A, fig. S10A). Fmoc deprotection reactions were carried out using 20% *v*/*v* piperidine in *N*,*N*-dimethylformamide (DMF). Coupling reactions were carried out using Fmoc-protected amino acids with *O*-(6-chlorobenzotriazol-1-yl)-*N*,*N*,*N*′,*N*′-tetramethyluronium hexafluorophosphate (HCTU) as coupling agent and *N*,*N*-diisopropylethylamine (DIPEA) as activating agent. Cy5-Chol [Cy5-PEG4-PEG3-PEG4-Asp(OChol)-NH_2] was prepared by manual SPPS using Fmoc-Asp(OChol)-OH, Fmoc-PEG4-OH, Fmoc-PEG3-OH, and Fmoc-PEG4-OH as the amino acids. After the final deprotection step, the *N*-terminus was capped using a mixture of Cy5 acid, HCTU, and DIPEA in DMF, and the peptide construct was then cleaved from resin using 95:2.5:2.5 trifluoroacetic acid (TFA)/triisopropylsilane (TIPS)/water. Cy5-Ethyl ester [Cy5-PEG4-PEG3-PEG4-Asp(OEt)-NH_2] was prepared as for Cy5-Chol, except for replacement of Fmoc-Asp(OChol)-OH with Fmoc-Asp(OEt)-OH in the first coupling step. Spantide I [^{D}Arg-Pro-Lys-

Pro-Gln-Gln-^{D}Trp-Phe-^{D}Trp-Leu-Leu-NH_2] was prepared by automated SPPS using the appropriate side-chain protected Fmoc-amino acids. After the final deprotection step, a portion of the material was cleaved from resin using 92.5:2.5:2.5:2.5 TFA/TIPS/1,2-ethanedithiol (EDT)/water and suspended in a 1:1 mixture of acetonitrile (ACN)/water containing 0.1% TFA to ensure complete side-chain deprotection. Spantide-cholestanol [Ac-Asp(OChol)-PEG4-PEG3-PEG4-Spantide-NH_2] was prepared from resin-bound spantide I by manual SPPS using Fmoc-PEG4-OH, Fmoc-PEG3-OH, Fmoc-PEG4-OH, and Fmoc-Asp(OChol)-OH as the amino acids (fig. S9A). After the final deprotection step, the *N*-terminus was capped using a mixture of acetic anhydride and DIPEA in DMF, and the peptide construct was then cleaved from resin using 92.5:2.5:2.5:2.5 TFA/TIPS/EDT/water. Spantide-ethyl ester [Ac-Asp(OEt)-PEG4-PEG3-PEG4-Spantide-NH_2] was prepared as for spantide-cholestanol, except for replacement of Fmoc-Asp(OChol)-OH with Fmoc-Asp(OEt)-OH in the final coupling step (fig. S9A). L-733,060-cholestanol [L-733,060-C8-PEG4-PEG3-PEG4-Asp(OChol)-NH_2] was prepared by manual SPPS using Fmoc-Asp(OChol)-OH, Fmoc-PEG4-OH, Fmoc-PEG3-OH, and Fmoc-PEG4-OH as the amino acids, respectively (fig. S10A). After the final deprotection step, the *N*-terminus was extended by coupling with 8-bromooctanoic acid, HCTU and DIPEA in DMF for 45 minutes. Finally, the bromo-terminated peptide was coupled with L-733,060·HCl, TBAI, and DIPEA for three days, and the construct was then cleaved from resin using 95:2.5:2.5 TFA/TIPS/water. *Purification and LC-MS analysis:* Constructs were purified by reverse-phase high-performance liquid chromatography (HPLC) using a Luna 5 μm C8, 250 × 21.2 mm column (Phenomenex), eluting with gradient mixtures of 0.1% TFA/water and 0.1% TFA/ACN, at a flow rate of 20 ml/min and detection at 214 and 254 nm. Combined fractions were freeze-dried for two days to give the target peptides as TFA salts with 5-10% overall yield (based on initial resin loading).

The identity of the final products were confirmed by liquid chromatography-mass spectrometry (LC-MS) using a Luna 3 μm C8(2), 100 × 2.0 mm column (Phenomenex), eluting with gradient mixtures of 0.05% TFA/water and 0.05% TFA/ACN, at a flow rate of 0.2 ml/min and detection at 214 nm. Mass spectra were acquired in positive ion mode with a scan range of 200-2000 *m/z*. *Spantide I:* gradient = 0-80% ACN over 25 min; t_R = 15.1 min; calcd for $C_{75}H_{110}N_{20}O_{13}$ [M + $2H^+$] *m/z* 749.90; obs. *m/z* 749.95. *Spantide-cholestanol:* gradient = 20-100% ACN over 20 min; t_R = 14.9 min; calcd for $C_{139}H_{223}N_{24}O_{31}$ [M + $3H^+$] *m/z* 908.80; obs. *m/z* 908.95 (fig. S9B). *Spantide-ethyl ester:* gradient = 0-60% ACN over 20 min; t_R = 14.8 min; calcd for $C_{114}H_{181}N_{24}O_{31}$ [M + $3H^+$] *m/z* 794.60; obs. *m/z* 794.90 (fig. S9C). *L-733,060-cholestanol:* gradient = 60-100% ACN over 20 min; t_R = 16.1 min; calcd. for $C_{90}H_{144}F_6N_6O_{19}$ $[M + 2H]^{2+}$ *m/z* 865.05, obs. *m/z* 865.35 (fig. S10B).

Alexa568-SP. AlexaFluor568 NHS ester (Invitrogen; 6.3 μmol) was incubated with SP (1.48 μmol) and triethylamine (2.9 μmol) in DMF (500 μl) (15 h, room temperature, RT). Alexa568-SP was purified by reverse-phase HPLC. The product was confirmed by mass spectrometry: *m/z* 1012.8, calcd for $C_{96}H_{127}N_{19}O_{24}S_3$ [M + $2H^+$] *m/z* 1012.9.

Cell-penetrating NK_1R peptides. Putative GRK2 phosphorylation sites within the intracellular C-terminus of the mouse NK_1R were predicted using Group Based Prediction System (http://gps.biocuckoo.org/wsresult.php?p=1). Peptides corresponding to these domains (S^{398}SSFYSNM^{405}, S^{390}NSKTMTE^{397}, L^{382}TSNGSSR^{389}) or control peptide (MSNSYSFS) with the N-terminal Tat membrane permeant sequence (YGRKKRRQRRR) were from American Peptide Company.

cDNAs. BRET probes NK_1R-RLUC8, KRas-Venus, RAB5A-Venus, βARR1-YFP, βARR2-YFP, $G\alpha_q$-RLUC8, and $G\gamma_2$-Venus have been described (*37, 38*). CytoEKAR and NucEKAR

(*39*) and CytoCKAR and pmCKAR (*40*) were from Addgene (plasmids 18680, 18681, 14870, 14862, respectively). CytoEpac2-camps (*41*) was from M. Lohse (University of Wurzburg) and pmEpac2-camps (*42*) was from D. Cooper (University of Cambridge). GFP-dynamin and GFP-dynamin K44E have been described (*19*). Human NK_1R with extracellular N-terminal Snap-Tag was from Cisbio. Full length and truncated δ311 rat HA-NK_1R have been described (*43*). RLUC8 fusions of these constructs were generated by removal of the stop codon by PCR and subcloning into a pcDNA3.1-RLUC8 vector.

Cell lines, transfection. HEK293 cells stably expressing rat or human NK_1R with N-terminal HA11 epitope have been described (*29*). HEK293 cells were grown in 6-well plates and transiently transfected using polyethylenimine (Polysciences) or FuGene (Promega) (*23*). Cells were grown in Dulbecco's modified Eagle's medium (DMEM) supplemented with 5% FBS (37°C, 5% CO_2). Cells were routinely checked for mycoplasma infection.

BRET. HEK293 cells were transfected with the following cDNAs (per well): 1 µg NK_1R-RLUC8 + 4 µg KRas-Venus, 4 µg RAB5A-Venus, 4 µg βARR1-YFP, or 4 µg βARR2-YFP; or 1 µg NK_1R + 0.5 µg $G\alpha_q$-RLUC8 + 1 µg $G\beta_1$ + 4 µg $G\gamma_2$-Venus; or 1 µg NK_1R + 0.5 µg $G\alpha_q$-RLUC8 + 1 µg $G\beta_1$ + 1 µg $G\gamma_2$ + 4 µg RAB5A-Venus. After 48 h, cells were equilibrated in Hank's balanced salt solution (HBSS) at 37°C, and incubated with the RLuc substrate coelenterazine h (5 µM, 15 min). BRET ratios were determined using a microplate reader LUMIstar Omega (BMG LabTech) before and after challenge with SP (0.1-10 nM) or vehicle (dH_2O) (*23*).

FRET biosensors of compartmentalized signaling. HEK293 cells were transfected with 55 ng/well rat NK_1R with N-terminal HA.11 epitope tag (HA-NK_1R) and 40 ng/well FRET biosensors. FRET was assessed 48 h after transfection, after serum restriction (0.5% FBS

overnight). For experiments using clathrin or dynamin siRNA, cells were transfected with 55 ng/well rat HA-NK_1R, 40 ng/well FRET biosensor, and 25 nM scrambled (control), clathrin heavy chain (Product #67300), or dynamin-1 (Product #13429) ON-TARGETplus SMARTpool siRNA (GE Dharmacon). FRET was assessed 72 h after transfection, after serum restriction (0.5% FBS overnight). Cells were equilibrated in HBSS at 37°C, and FRET was analyzed using a GE Healthcare INCell 2000 Analyzer (*20*, *23*). For GFP/RFP emission ratio analysis, cells were sequentially excited using a FITC filter (490/20) with emission measured using dsRed (605/52) and FITC (525/36) filters, and a polychroic filter set optimized for the FITC/dsRed (Quad4). For CFP/YFP emission ratio analysis, cells were sequentially excited using a CFP filter (430/24) with emission measured using YFP (535/30) and CFP (470/24) filters, and a polychroic filter set optimized for the CFP/YFP (Quad3). Cells were imaged every 1 min, allowing image capture of 14 wells per minute. Baseline emission ratio images were captured for 4 min. Cells were challenged with an EC_{50} concentration of SP (1 nM) or vehicle, and images were captured for 20 min. Cells were then stimulated with the positive control (200 nM phorbol 12,13-dibutyrate for ERK; 200 nM phorbol 12,13-dibutyrate with phosphatase inhibitor cocktail for PKC; 10 μM forskolin, 100 μM 3-isobutyl-1-methylxanthine, 100 nM PGE_1 for cAMP) for 10 min to generate a maximal increase, and positive emission ratio images were captured for 4 min. Data were analyzed as described and expressed as emission ratios relative to baseline for each cell (F/F_0) (*20*, *23*). Cells with >10% change in F/F_0 after stimulation with positive controls were selected for analysis.

FRET assays of endosomal NK_1R targeting. HEK293 cells were transfected with 50 ng/well of human NK_1R with extracellular N-terminal SNAP-Tag. After 48 h, the cell-surface NK_1R was labeled with SNAP-Surface 549 photostable fluorescent substrate (New England Biolabs) (1 μM, 30

min, 37°C in DMEM, 0.5% BSA). Cells were washed, recovered in DMEM for 30 min, and stimulated with SP (10 nM, 30 min, 37°C) to induce NK_1R endocytosis. Cells were incubated with Cy5-Chol (200 nM, 37°C). SNAP-549/Cy5 sensitized emission FRET was analyzed by confocal microscopy using sequential excitation with Argon (514 nm)/HeNe (633 nm) lasers and emission at 570-620 nm (SNAP-549 donor) and 670-750 nm (Cy5 FRET and Cy5 acceptor) before (F_0) and after (F) addition of Cy5-Chol. Untransfected HEK293 cells (acceptor only) were used as controls. To measure FRET within the cytosol (in endosomes), a region of interest was drawn in the cytosol to exclude the plasma membrane. FRET was measured in the region of interest, and expressed as emission ratios relative to controls (F/F_0). Results are from N=3 separate experiments, with 7-9 cells analyzed per experiment.

Transcription assays. HEK293 cells were transfected with 70 ng/well human or rat NK_1R or $NK_1R\delta311$ and 250 ng/well secreted alkaline phosphatase (SEAP) reporter gene under the control of the specific transcription factor consensus sequence for Serum-Response Element (SRE) (*44*). Some cells were also transfected with 70 ng/well dynamin WT, dynamin K44E, or pcDNA3. After 24 h, cells were placed in phenol-red free DMEM containing 0.5% FBS, 1 mM sodium pyruvate, and 50 units/ml penicillin/streptomycin. The following day, a sample of medium was collected from each well. Cells were then stimulated with vehicle or SP (0.1-100 nM) for 4 or 20 h before collection of a second sample. Samples (5 µl) were mixed with SEAP buffer (45 µl, 2 M diethanolamine, 1 mM $MgCl_2$, pH 10.3) and heat-treated (65°C, 30 min) to denature any endogenous alkaline phosphatases. Samples were cooled to room temperature, mixed with SEAP substrate (5 µl 2 mM 4-methylumbelliferyl phosphate in SEAP buffer). After 1 h of incubation in the dark, the fluorescence intensity (Ex/Em = 360 nm/440 nm) was

measured. The data were analyzed by subtracting the basal from the SP-stimulated SEAP secretion.

Ca^{2+} assays. $[Ca^{2+}]_i$ was measured as described (*23*). HEK293 cells transiently expressing HA-NK_1R or HA-CLR/Myc-RAMP1 were loaded with Fura2-AM (2 μM). To compare the antagonistic capacity of Span and Span-Chol, cells were preincubated for 30 min with antagonists, and then challenged with SP (3 nM, EC_{80}). L-733,060 and L-733,060-Chol (10 nM) were similarly tested for their ability to inhibit SP (1 nM)-stimulated Ca^{2+} signals.

Cell-surface ELISA. HEK293 cells transiently transfected with HA-NK_1R or HA-$NK_1R\delta311$ were fixed in 4% paraformaldehyde, 100 mM PBS pH 7.4 (PFA, 30 min, 4°C). For analysis of total expression, cells were permeabilized using 0.5% NP-40 in TBS (30 min) after fixation. Cells were incubated in blocking buffer (1% skim milk powder, 0.1 M $NaHCO_3$, 4 h, RT), and then anti-HA (1:5,000, Sigma; overnight, 4°C). Cells were washed and incubated with anti-mouse horseradish peroxidase-conjugated antibody (1:2,000, 2 h, RT). Cells were washed and stained using the SIGMAFAST substrate (SigmaAldrich). Absorbance at 490 nm was measured using an EnVision plate reader (PerkinElmer Life Sciences). Values were normalized to HEK293 cells transfected with pcDNA3 or to untreated cells.

NK_1R trafficking in cell lines. HEK-NK_1R cells were plated on poly-D-Lysine coated glass chamber slides or coverslips and cultured for 48 h. To examine uptake of fluorescent SP, cells were incubated in HBSS with Alexa568-SP (100 nM, 20 min, 4°C), washed, incubated for 30 min at 37°C, and fixed in PFA. Cells were examined by confocal microscopy. To examine NK_1R and $G\alpha_q$ trafficking, cells were incubated in HBSS with SP (100 nM, 15 min) or vehicle and fixed. Cells were blocked in PBS, 0.2% saponin, 3% normal goat serum (1 h, RT). Cells were incubated in primary antibodies: rat anti-HA (1:1,000; Roche), rabbit anti-$G\alpha_q$ (1:2,000, C-19;

Santa Cruz Biotechnology), mouse anti-EEA1 (1:100, 610457; BD Biosciences) (overnight, 4°C). Cells were washed and incubated with donkey anti-rat Alexa488 (1:500), donkey anti-rabbit Alexa568 (1:1,000), and donkey anti-mouse Alexa647 (1:1,000) (Life Technologies or Jackson ImmunoResearch) (1 h, RT). Cells were examined by super-resolution microscopy.

Inhibitors. HEK293 cells were preincubated for 30 min with 30 μM each of Dy4, Dy4 inactive (*17*), PS2, PS2 inactive (*18*), 100 nM UBO-QIC (Institute of Pharmaceutical Biology, University of Bonn, Germany), 1 μM U73122, 10 μM NF449 (Merck Millipore), 1 μM GF109203X, 100 μM EGTA, 30 μM each of cell-penetrating NK_1R peptides (Tat-conjugated $S^{398}SSFYSNM^{405}$, $S^{390}NSKTMTE^{397}$, $L^{382}TSNGSSR^{389}$), 100 μM control peptide (Tat-conjugated MSNSYSFS), or vehicle (dH_2O or 0.1% DMSO). Pitstop and Dyngo are trademarks of Children's Medical Research Institute, Newcastle Innovation, and Freie Universitat Berlin.

Cy5 tripartite probe uptake. HEK293 cells were plated on poly-D-lysine-coated glass coverslips. Cells were infected with CellLight RAB5A-RFP (Life Technologies) or were transfected with rat NK_1R-GFP. After 24 h, cells were equilibrated in HBSS, imaged at 37°C by confocal microscopy, and incubated with Cy5-Chol, Cy5-Ethyl ester, or Cy5-Span-Chol (1.5 μM). Cells expressing NK_1R-GFP were incubated with SP (10 nM).

Spinal cord slices. Parasagittal slices (340-400 μm) were prepared using a vibratome from the lumbar region of the rat spinal cord in ice-cold sucrose-based artificial CSF (sACSF) (mM: 100 sucrose, 63 NaCl, 2.5 KCl, 1.2 NaH_2PO_4, 1.2 $MgCl_2$, 25 glucose, 25 $NaHCO_3$; 95% O_2/5% CO_2). Slices were transferred to N-Methyl-D-Glucamine (NMDG)-based recovery ACSF (rACSF) (mM: 93 NMDG, 93 HCl, 2.5 KCl, 1.2 NaH_2PO_4, 30 $NaHCO_3$, 20 HEPES, 25 glucose, 5 Na ascorbate, 2 thiourea, 3 Na pyruvate, 10 $MgSO_4$, 0.5 $CaCl_2$; 95% O_2/5% CO_2, 15 min, 34°C). Slices were transferred to normal ACSF (mM: 125 NaCl, 2.5 KCl, 1.25 NaH_2PO_4, 1.2 $MgCl_2$,

2.5 $CaCl_2$, 25 glucose, 11 $NaHCO_3$; 95% O_2/5% CO_2) containing 10 μM MK-801 (45 min, 34°C), then maintained at RT.

Electrophysiology. Slices of rat spinal cord were transferred to a recording chamber and superfused with normal ACSF (2 ml/min, 36°C). Dodt-contrast optics were used to identify large (capacitance ≥ 20 pF), putative NK_1R-positive neurons in lamina I based on their position, size, and fusiform shape with dendrites that were restricted to lamina I (*45*). Slices were preincubated with Dy4 or Dy4 inact (30 μM, 0.03% DMSO) for 10 min before recording, or were preincubated with Span-Chol or Span (1 μM, 0.01% DMSO) for 60 min, washed, and incubated in antagonist-free ACSF for a further 60 min before recording. PS2 was not soluble in the low concentrations of DMSO required for electrophysiology. To investigate the signaling mechanisms underlying excitation, slices were incubated with the MEK inhibitor U0126 or the PKC inhibitor GFX109203X (1 μM, 0.01% DMSO) for 30-45 min before recording. Large, NK_1R-positive, presumed nociceptive lamina I neurons were visually identified as described (*46*). Spontaneous currents were recorded in cell-attached configuration (Multiclamp 700B, Molecular Devices), sampled at 10 kHz, high pass filtered at 1 Hz, and capacitatively coupled action potential events were analyzed using Axograph X, V 1.4.4 (Axograph). Patch electrodes (resistance 2.5-3.5 MΩ) contained KMES-based internal solution (mM: 105 KMES, 20 NaCl, 5 HEPES, 10 BAPTA, 1.5 $MgCl_2$, 4 MgATP, 0.4 NaGTP, 0.1% biocytin; 285-295 mosmol/l) to facilitate subsequent recordings of action potential properties in whole-cell configuration. Recordings were made in the presence of CNQX (6-cyano-7-nitroquinoxaline-2,3-dione) (10 μM; AMPA/kainate receptor antagonist), picrotoxin (100 μM; $GABA_A$ receptor antagonist), strychnine (0.5 μM; glycine and acetylcholine receptor antagonist), and AP5 ((2*R*)-amino-5-phosphonovaleric acid; (2*R*)-amino-5-phosphonopentanoate) (100 μM; NMDA receptor

antagonist) to minimize presynaptic influences on action potential properties. Slices were challenged by superfusion with SP (1 μM) for 2 min. Recordings were sampled at 10 kHz and filtered with a high pass filter at 1 Hz, and firing rate was measured in two-minute interval bins. At the end of each cell-attached recording, whole-cell recordings were made in current-clamp mode to confirm retention of normal action potential firing. Data were only included in the analysis if cells had action potential amplitudes that were ≥50 mV above threshold to ensure viable neurons were included. Cells were filled with biocytin, and sections were processed to confirm NK_1R expression by immunofluorescence. The firing rate for each cell was normalized to the response at the 2 min time point, which was not significantly different between groups. The firing time was determined as the duration of the response to last action potential. To assess synaptic transmission, whole-cell configuration recordings were made under control conditions or after exposure to Dy4 or Dy4 inact; a bipolar stimulating electrode was placed at the dorsal root entry zone, and electrically-evoked excitatory postsynaptic currents recorded as described (*46*). To assess NK_1R endocytosis, spinal cord slices (400 μm) were incubated with SP (1 μM, 5 min), fixed in PFA (4 h, RT), cryoprotected, and were processed to localize NK_1R.

Neuropeptide release. Slices (0.4 mm) of mouse dorsal spinal cord (combined cervical, thoracic, lumbar-sacral segments) were superfused (0.4 ml/min) with Krebs' solution (mM: NaCl 119, $NaHCO_3$ 25, KH_2PO_4 1.2, $MgSO_4$ 1.5, $CaCl_2$ 2.5, KCl 4.7, D-glucose 11 mM; 95% CO_2/5% O_2, 37°C) containing 0.1% BSA, 1 μM phosphoramidon, and 1 μM captopril (*47*). Tissues were superfused with Dy4, PS2, inactive analogues (30 μM), or vehicle (0.3% DMSO/saline) for 30 min. Tissues were then superfused with capsaicin (0.3 μM, 10 min) in the presence of inhibitors or controls. Superfusate (10 min collections, 4 ml) was collected before, during, and after capsaicin stimulation, and analyzed for SP-IR and CGRP-IR (Bertin Pharma).

Endocytic inhibitors did not interfere with immunoassays. Detection limits of the assays were 2 pg/ml for SP-IR and 5 pg/ml for CGRP-IR. Results are expressed as fmol/g/20 min.

NK_1R endocytosis in rat spinal neurons. Dy4, Dy4 inact, PS2, PS2 inact (all 50 µM), or vehicle (1% DMSO/saline) was injected intrathecally (10 µl, L3/L4) into conscious rats. After 30 min, rats were sedated (5% isoflurane) and capsaicin (12.5 µg) or vehicle (20% ethanol, 10% Tween 80, 70% saline) was injected subcutaneously into the plantar surface of one hindpaw (25 µl). After 10 min, rats were transcardially perfused with PBS and then 4% PFA. The spinal cord was removed, immersion-fixed in PFA (2 h, 4°C), and cryoprotected (30% sucrose, PBS, 24 h, 4°C). The spinal cord (T12 to L4) was embedded in OCT, and 30 µm serial coronal sections were cut into 48-well plates containing PBS. Free-floating sections were blocked in PBS containing 10% normal horse serum (1 h, RT). Sections were incubated with mouse anti-NeuN (1:20,000; AbCam) and either rabbit anti-NK_1R (*48*) (1:5,000, #94168) or rabbit anti-pERK (1:200; Cell Signaling Technology) in PBS containing 3% normal horse serum (48 h, 4°C). Sections were washed (4 x 20 min in PBS) and incubated with donkey anti-rabbit Alexa488 (1:2,000-1:8,000) and donkey anti-mouse Alexa568 (1:2,000 (Life Technologies) (1 h, RT). Sections were washed, incubated with DAPI (10 µg/ml, 5 min), and mounted in Vectashield (Vector Laboratories).

Nociception in mice and rats, NK_1R endocytosis in spinal neurons in mice. Mice and rats were acclimatized to the experimental apparatus and environment for 1-2 h on 2 successive days before experiments. Mechanical allodynia and hyperalgesia were assessed by paw withdrawal to stimulation of the plantar surface of the hind-paw with graded von Frey filaments (*49*). On the day before the study, von Frey scores were measured in triplicate to establish a baseline for each animal. To assess edema of the paw, hindpaw thickness was measured using digital calipers

before and after treatments (*50*). For intraplantar injections, mice and rats were sedated (5% isoflurane). Capsaicin (5 µg), Complete Freund's Adjuvant (CFA, 2 mg/ml), or vehicle (capsaicin: 20% ethanol, 10% Tween 80, 70% saline; CFA: saline) was injected subcutaneously into the plantar surface of the left hindpaw (10 µl). von Frey scores (left and right paws) and paw thickness (left paw) were measured at 30 or 60 min intervals from 30-240 min after capsaicin, and 36-42 h after injection of CFA. Results are expressed as percent pre-injected values. For assessment of nocifensive behavior, mice were sedated (5% isoflurane), and formalin (4%, 10 µl) was injected subcutaneously into the plantar surface of the left hindpaw. Mice were placed in a Perspex container, and nocifensive behavior (flinching, licking, biting of the injected paw) was recorded for 60 min. The total number of nocifensive events was subdivided into acute (I, 0-10 min) and tonic (II, 10-60 min) phases. At the end of experiments, mice were transcardially perfused with PBS and PFA, and the spinal cord was removed and processed to localize the NK_1R by immunofluorescence, as described for rats. Investigators were blinded to test agents.

Intrathecal injections in mice. Intrathecal injections (5 µl, L3/L4) were made into conscious mice. Dy4, Dy4 inact, PS2, PS2 inact (all 50 µM), SR-140333 (15 µM), SM-19712 (8 mM), U0126 (100 µM), 30 µM each of cell-penetrating NK_1R peptides (Tat-conjugated $S^{398}SSFYSNM^{405}$, $S^{390}NSKTMTE^{397}$, $L^{382}TSNGSSR^{389}$), 100 µM control peptide (Tat-conjugated MSNSYSFS), or vehicle (1% DMSO/saline) was injected intrathecally 30 min before intraplantar injection of capsaicin or formalin, or 36 h after CFA. Span (50 µM), Span-Chol (50 µM), L-733,060 (100 nM), L-733,060-Chol (100 nM), or Cy5-Chol (10 µM) was injected intrathecally 3 h before or 30 min after intraplantar injection of capsaicin, 3 h before formalin, or 36 h after CFA.

Intrathecal siRNA in mice. Cationic liposome and adjuvant anionic polymer (polyglutamate) were used to deliver siRNA (*51*). siRNA targeting mouse dynamin-1 (5' (S-S) UAA GUG UCA AUC UGG UCU C dTdT 3') or control siRNA (5' (S-S) CGU ACG CGG AAU ACU UCG AUU dTdT) (*52*), or siRNA targeting mouse βARR1 (sense 5' AGC CUU CUG CGC GGA GAA U dTdT 3', antisense 5' dTdT U CGG AAG ACG CGC CUC UUA 5') plus mouse βARR2 (sense: 5' CCU ACA GGG UCA AGG UGA A dT dT 3', antisense: 5' UUC ACC UUG ACC CUG UAG G dT dT 3') or control siRNA (sense: 5' AAG GCC AGA CGC GAA UUA U dT dT, 3' antisense: 5' AUA AUU CGC GUC UGG CCU U dT dT 3') (Dharmacon) (50 ng, 0.5 µl of 100 ng.µl^{-1} stock) was mixed with 0.5 µl of adjuvant polyglutamate (0.1 µg/µl stock) and 1.5 µl sterile 0.15 M NaCl. Liposome solution, cationic lipid 2- {3-[bis-(3-amino-propyl)-amino]-propylamino}-N-ditetradecylcarbamoylmethyl-acetamide (DMAPAP) and L-α-dioleoyl phosphatidylethanolamine (DOPE) (DMAPAP/DOPE, 1/1 M:M) (2.5 µl of 200 µM) was added to siRNA/adjuvant, vortexed for 1 min, and incubated (30 min, RT). The siRNA lipoplexes were administered to mice by intrathecal injection (L1-L4, 5 µl). After behavioral testing (24-48 h), the spinal cord (L1-L4) was collected for analysis of dynamin-1 expression by Western blotting and βARR1 and βARR2 expression by q-PCR.

Western blotting. *Cell lines.* HEK293 cells were lysed in 150 µl of RIPA buffer containing HALT protease and phosphatase inhibitors (Thermo Scientific). Samples were sonicated on ice, centrifuged, and supernatant (20 µg protein) was fractionated by 10% SDS-PAGE and transferred to PVDF membranes. Membranes were blocked (1 h, RT) in Odyssey blocking buffer (LI-COR Biosciences), and incubated with sheep anti-dynamin-1 (*53*) (1:1,000) or rabbit anti-clathrin (1 µg/ml, AbCam) antibodies in PBS, 0.2% Tween-20, 50% Odyssey blocking buffer (16 h, 4°C). Membranes were washed and incubated with donkey anti-goat 680 or goat anti-

rabbit 680 (1:10,000; LI-COR Biosciences) (1 h, RT). Membranes were washed and imaged with the LI-COR Odyssey infrared scanner. Membranes were stripped and re-probed with rabbit anti-β-actin (1:1,000; Cell Signaling Technology, 16 h, 4°C), washed, incubated with goat anti-rabbit 800 (1:10,000, 1 h at RT, LI-COR), and re-imaged. Signals were quantified using ImageJ (NIH).

Spinal cord. The dorsal half of the spinal cord was placed in 100 µl of ice-cold RIPA buffer containing HALT protease and phosphatase inhibitors (Thermo Scientific). Tissues were homogenized, centrifuged, and supernatant (20 µg protein) was separated by 10% SDS-PAGE and transferred to PVDF membranes. Membranes were processed to detect dynamin-1 and β-actin as described above.

q-PCR. Mouse lumbar spinal cord (L1-L4) was placed in RNA*later* (Qiagen), and total RNA was isolated using RNeasy RNA Isolation kit (Qiagen). Total RNA (500 ng) was reverse-transcribed using Superscript III cDNA Synthesis Kit (Invitrogen). cDNA was amplified using Eppendorf RealPlex Real Time PCR System. Twenty microliters of amplification reaction included cDNA template, TaqMan Universal Master Mix, and TaqMan Gene Expression Assays for one of the following genes (catalog no.): *Arrb2* (Mm00520666_g1), *Arrb1* (Mm00617540_m1), *Actb* (Mm02619580_g1), *Gapdh* (hs00363153_m1). Samples were amplified in triplicates. For real-time quantitative PCR, the ΔΔCt method (Applied Biosystems) was used to calculate relative changes in mRNA abundance. The threshold cycle (Ct) values for the housekeeping genes *Actb* and *Gapdh* were subtracted from the Ct value for the gene of interest (Δ*C*t). Data were expressed as relative abundance using the equation: $2^{-\Delta Ct} * 1000$, where $\Delta Ct = Ct_{\text{gene of interest}} - Ct_{Actb,Gapdh}$. The results are presented as mRNA abundance (fold-change or percentage of housekeeping genes).

Rotarod latency. Mice were acclimatized by three trials on two successive days before experiments. Mice were trained to remain on the rotarod for three consecutive periods. On the experimental day, three baseline time trials (cut-off 120 s) were recorded. Dy4, PS2, inactive analogues (50 µM), or vehicle was injected intrathecally (5 µl, L3/L4). After 30 min, mice were placed on the rotarod with accelerating velocity for up to 120 s. Times were recorded in three successive trials, and latency time to fall was determined at 30, 90, and 120 min.

Confocal microscopy, image analysis. Tissues and cells were examined using a Leica SP8 confocal microscope using HCX PL APO 40x (NA 1.30) and HCX PL APO 63x (NA 1.40) oil objectives. Z stacks were collected of NK_1R-positive neurons in lamina I of the dorsal horn. Video projections of Z stacks were made using Imaris Software (Bitplane). NK_1R endocytosis and pERK expression were quantified using ImageJ. To quantify NK_1R internalization in lamina I neurons, the border of the cytoplasm of the neuronal soma was defined by NeuN fluorescence, and NK_1R fluorescence within 5 pixels (0.5 µm) of the border was defined as plasma membrane-associated receptor. The ratio of plasma membrane to cytosolic NK_1R-IR fluorescence was determined in ≥6 lamina I neurons per animal per condition. To quantify ERK activation, the ratio of the number of pERK-IR neurons to total NeuN-N-positive neurons in lamina I was determined in ≥6 fields (x40 objective) per condition.

Super-resolution microscopy. Coverslips were mounted and sealed on a concave slide containing 100 mM cysteamine (MEA). Cells were observed using a Leica DMI6000 Ground State Depletion microscope with a HCX PL APO 100x (NA 1.49) objective, a SuMo Stage, an Andor iXon 3 897 camera using LAS AF software (version 3.2.0.9652, Leica). Fluorophores were imaged sequentially starting with the 647 channel to avoid photo bleaching of lower wavelength channels. Pumping occurred at 100% laser power for each fluorophore until the

frame correlation dropped to <0.2. Channels were acquired at 50% laser power, and 27,000-30,000 frames per channel were captured. The number of EEA-IR endosomes per cell containing NK_1-IR and $G\alpha_q$-IR was determined. A 300 nm diameter region of interest (average size of EEA1 positive structures) was drawn around all EEA1-IR endosomes in an image using ImageJ. The proportion of regions of interest that contained detectable NK_1R-IR and $G\alpha_q$-IR was determined. Results are expressed as the percentage of EEA1-IR endosomes containing NK_1R-IR, $G\alpha_q$-IR, or both NK_1R-IR and $G\alpha_q$-IR. Images were analyzed from 20 (SP, 37°C) or 22 (SP, 4°C) cells.

Metabolic stability of tripartite probes. Membranes were prepared from mouse spinal cord as described (*54*), with final centrifugation at 40,000 *g*. Normal human cerebrospinal fluid was provided by Dr. Paul Myles, Alfred Hospital Melbourne. To assess stability, SP, Span, or Span-Chol (10 $\mu g.ml^{-1}$) was incubated with mouse spinal cord membranes (40 µg/ml protein) or human cerebrospinal fluid (0-4 h, 37°C), and then snap frozen. Proteins were precipitated using ACN. Samples were analyzed by LC/MS using a Waters Xevo TQ triple quadrupole mass spectrometer coupled to a Waters Acquity UPLC. Chromatographic separation of peptides was achieved on a Merck Millipore Chromolith RP-18e monolithic column (50 x 2 mm; mouse spinal membranes) or a Supelco Ascentis Express Peptide ES C18 column (50 x 2.1 mm, 2.7 µm particle size; human cerebrospinal fluid) using 0.05% formic acid in H_2O and ACN as solvents. Peptides were quantified using positive electrospray ionization by comparison to a calibration standard (10-20,000 ng/ml) and by Multiple Reaction Monitoring using an internal standard (6.25 ng/ml diazepam in 50% ACN-water).

Statistical analyses. Data are presented as mean±SEM, unless noted otherwise. Table S1 indicates the statistical tests and the cell replicates for each figure.

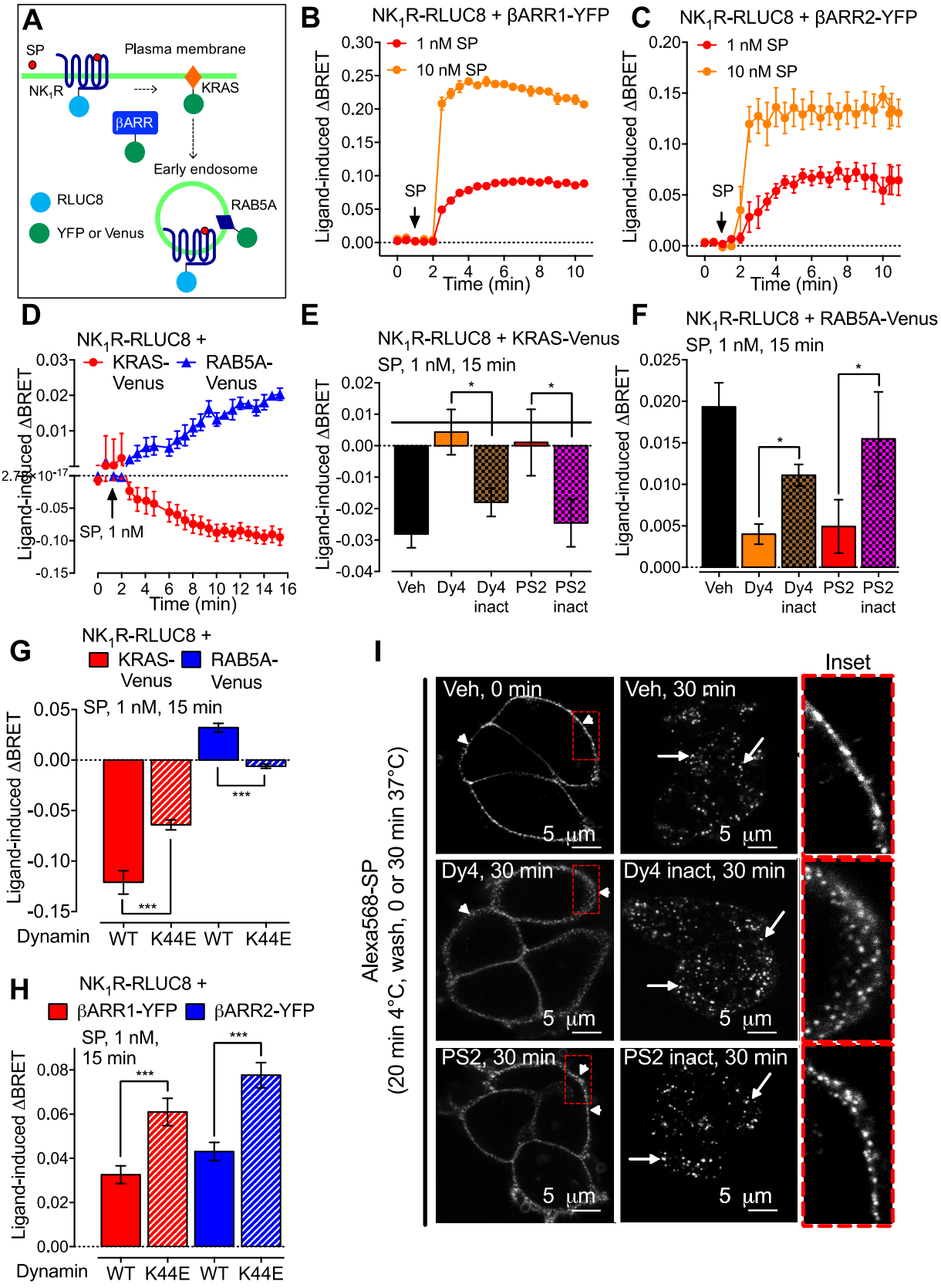
A
SP
Plasma membrane
NK1R
KRAS
βARR
Early endosome
RLUC8
RAB5A
YFP or Venus
B
NK1R-RLUC8 + βARR1-YFP
1 nM SP
10 nM SP
Ligand-induced ΔBRET
SP
Time (min)
C
NK1R-RLUC8 + βARR2-YFP
1 nM SP
10 nM SP
Ligand-induced ΔBRET
SP
Time (min)
D
NK1R-RLUC8 +
KRAS-Venus
RAB5A-Venus
Ligand-induced ΔBRET
SP, 1 nM
Time (min)
E
NK1R-RLUC8 + KRAS-Venus
SP, 1 nM, 15 min
Ligand-induced ΔBRET
Veh
Dy4
Dy4 inact
PS2
PS2 inact
F
NK1R-RLUC8 + RAB5A-Venus
SP, 1 nM, 15 min
Ligand-induced ΔBRET
Veh
Dy4
Dy4 inact
PS2
PS2 inact
G
NK1R-RLUC8 +
KRAS-Venus
RAB5A-Venus
SP, 1 nM, 15 min
Ligand-induced ΔBRET
Dynamin
WT
K44E
WT
K44E
H
NK1R-RLUC8 +
βARR1-YFP
βARR2-YFP
SP, 1 nM, 15 min
Ligand-induced ΔBRET
Dynamin
WT
K44E
WT
K44E
I
Inset
Alexa568-SP
(20 min 4°C, wash, 0 or 30 min 37°C)
Veh, 0 min
Veh, 30 min
Dy4, 30 min
Dy4 inact, 30 min
PS2, 30 min
PS2 inact, 30 min
5 μm

Fig. S1. Clathrin- and dynamin-dependent NK_1R endocytosis. A. Schematic of BRET assays for βARR recruitment and NK_1R trafficking. **B** to **D.** SP (1 or 10 nM) -induced changes in BRET between NK_1R-RLUC8 and βARR1-YFP (**B**), βARR2-YFP (**C**), KRAS-Venus (**D**), or RAB5A-Venus (**D**) in HEK293 cells. **E** to **H.** Effects of inhibitors of dynamin (Dyngo4a; Dy4) or clathrin (Pitstop-2; PS2), inactive (inact) analogues, or dominant negative dynamin K44E (K44E) and wild-type (WT) dynamin on SP-induced changes in BRET between NK_1R-RLUC8 and KRas-Venus (**E** and **G**), or RAB5A-Venus (**F** and **G**), or βARR2-YFP (**H**) at 15 min. **I.** Alexa568-SP endocytosis in HEK-NK_1R cells preincubated with vehicle (Veh), Dy4, PS2, or inactive analogues. Arrowheads, cell surface; arrows, endosomes. $*P<0.05$, $**P<0.01$, $***P<0.001$. Triplicate observations, $N\geq3$ experiments. ANOVA, Dunnett's test (E-H).

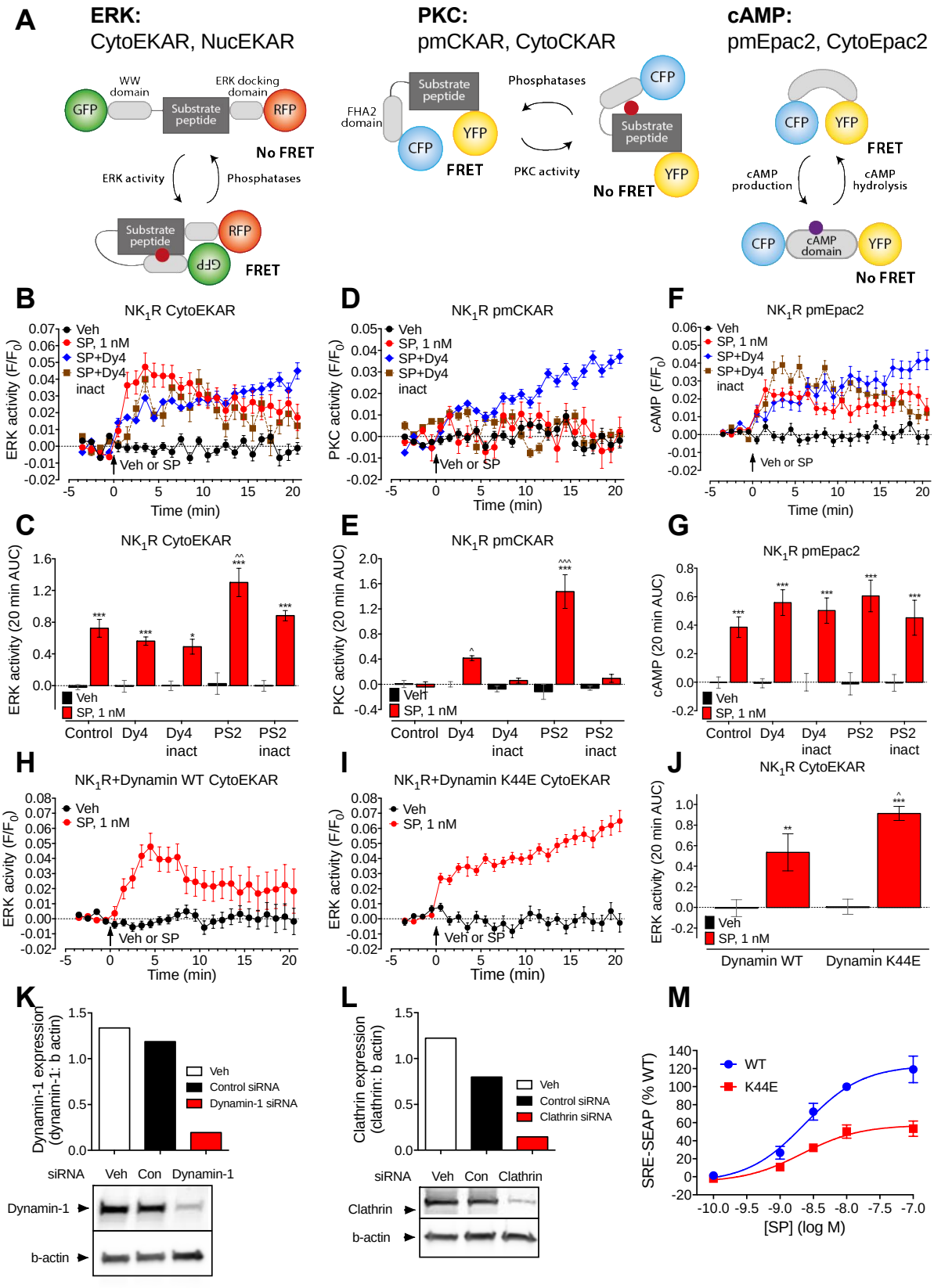
A
ERK:
CytoEKAR, NucEKAR
WW domain
ERK docking domain
GFP
Substrate peptide
RFP
No FRET
ERK activity
Phosphatases
FRET
PKC:
pmCKAR, CytoCKAR
FHA2 domain
Phosphatases
PKC activity
cAMP:
pmEpac2, CytoEpac2
cAMP production
cAMP hydrolysis
cAMP domain
CFP
YFP
B
NK1R CytoEKAR
ERK activity (F/F0)
Veh
SP, 1 nM
SP+Dy4
SP+Dy4 inact
Veh or SP
Time (min)
C
NK1R CytoEKAR
ERK activity (20 min AUC)
Control
Dy4
Dy4 inact
PS2
PS2 inact
D
NK1R pmCKAR
PKC activity (F/F0)
E
NK1R pmCKAR
PKC activity (20 min AUC)
F
NK1R pmEpac2
cAMP (F/F0)
G
NK1R pmEpac2
cAMP (20 min AUC)
H
NK1R+Dynamin WT CytoEKAR
I
NK1R+Dynamin K44E CytoEKAR
J
NK1R CytoEKAR
Dynamin WT
Dynamin K44E
K
Dynamin-1 expression (dynamin-1: b actin)
Control siRNA
Dynamin-1 siRNA
siRNA
Veh
Con
Dynamin-1
b-actin
L
Clathrin expression (clathrin: b actin)
Clathrin siRNA
Clathrin
M
SRE-SEAP (% WT)
WT
K44E
[SP] (log M)

Fig. S2. NK_1R compartmentalized signaling. A. Schematic of FRET biosensors for cytosolic (CytoEKAR) and nuclear (NucEKAR) ERK, plasma membrane (pmCKAR) and cytosolic (CytoCKAR) PKC, and plasma membrane (pmEpac2) and cytosolic (CytoEpac2) cAMP. **B** to **J.** FRET assays of compartmentalized signaling in HEK293 cells. **B** and **C.** Cytosolic ERK. **D** and **E.** Plasma membrane PKC. **F** and **G.** Plasma membrane cAMP. **B** to **F.** Effect of dynamin (Dy4) and clathrin (PS2) inhibitors and inactive (inact) analogues on the spatiotemporal profile of SP-induced signals. **C** to **G.** Area under the curve (AUC) analysis of data from **B** to **I.** Effect of dynamin WT (**H**) or dominant negative dynamin K44E (**I**) on the spatiotemporal profile of SP-induced activation of cytosolic ERK. **J.** AUC of **H** to **L.** siRNA knockdown of dynamin-1 (**K**) and clathrin heavy chain (**L**) (Western blots) in HEK293 cells. **M.** Effect of dynamin WT or dominant negative dynamin K44E on SRE-SEAP release 24 h after stimulation with graded concentrations of SP. **P*<0.05, ***P*<0.01, ****P*<0.001 SP to vehicle; ^*P*<0.05, ^^*P*<0.01, ^^^*P*<0.001 inhibitors to control. B-J, 16 to 354 cells, 3 experiments. ANOVA, Tukey's test (C, E, G); Sidak's test (J).

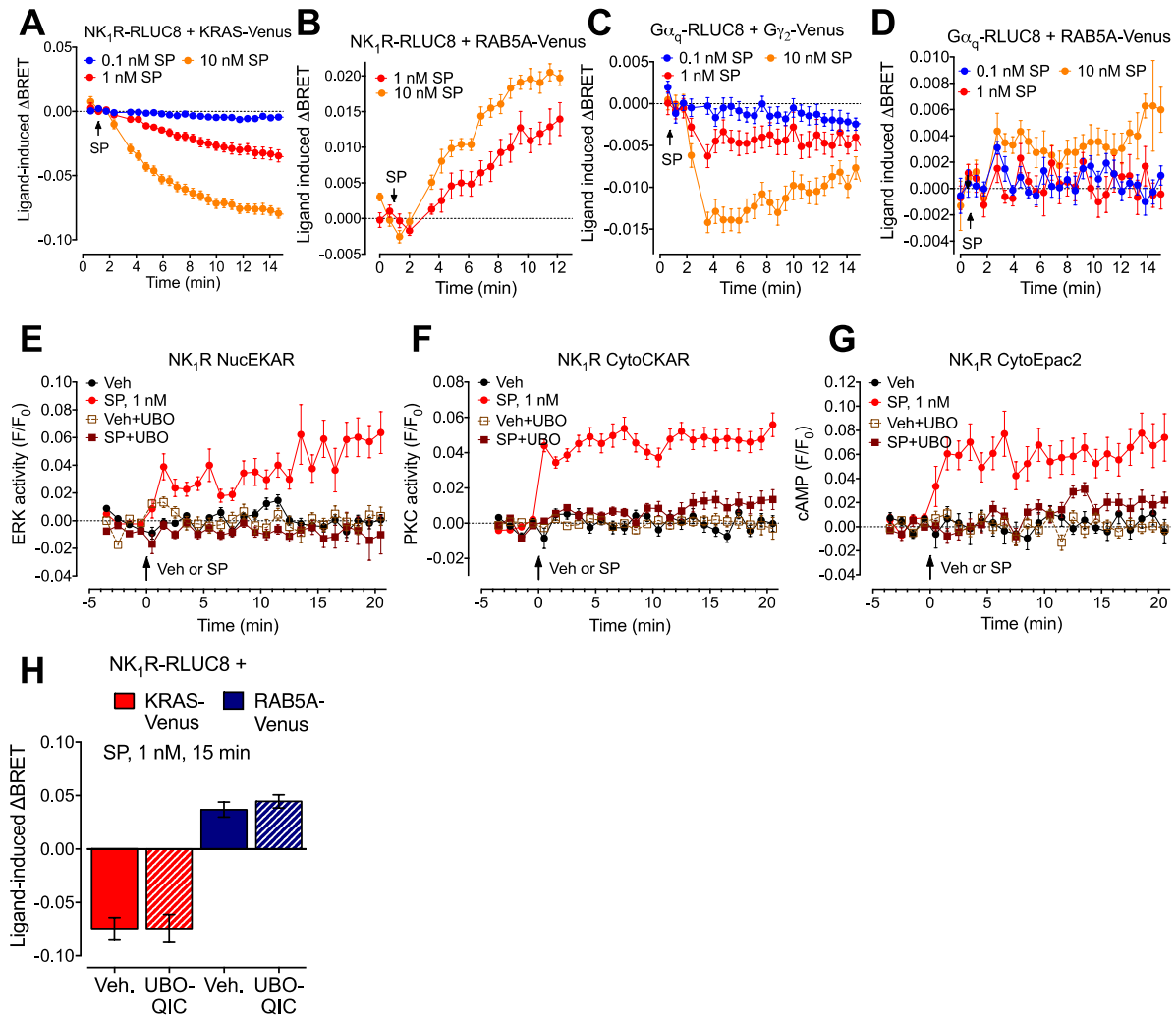

Fig. S3. G protein–dependent NK_1R signaling in endosomes. A to **D.** SP-induced BRET between NK_1R-RLUC8 and KRas-Venus (**A**) or RAB5A-Venus (**B**), and between $G\alpha_q$-RLUC8 and $G\gamma_2$-Venus (**C**) or RAB5A-Venus (**D**) in HEK293 cells. Triplicate observations, $N \geq 3$ experiments. **E** to **G.** Effect of $G\alpha_q$ inhibitor (UBO-QIC, UBO) on SP-induced spatiotemporal profiles of nuclear ERK (NucEKAR, **E**), cytosolic PKC (CytoCKAR, **F**), and cytosolic cAMP (CytoEpac2, **G**) measured in HEK293 cells using FRET biosensors. 35-67 cells, 3 experiments. **H.** SP-induced changes in BRET between NK_1R-RLUC8 and KRas-Venus or RAB5A-Venus in the absence (Veh) or presence of the $G\alpha_q$ inhibitor UBO-QIC.

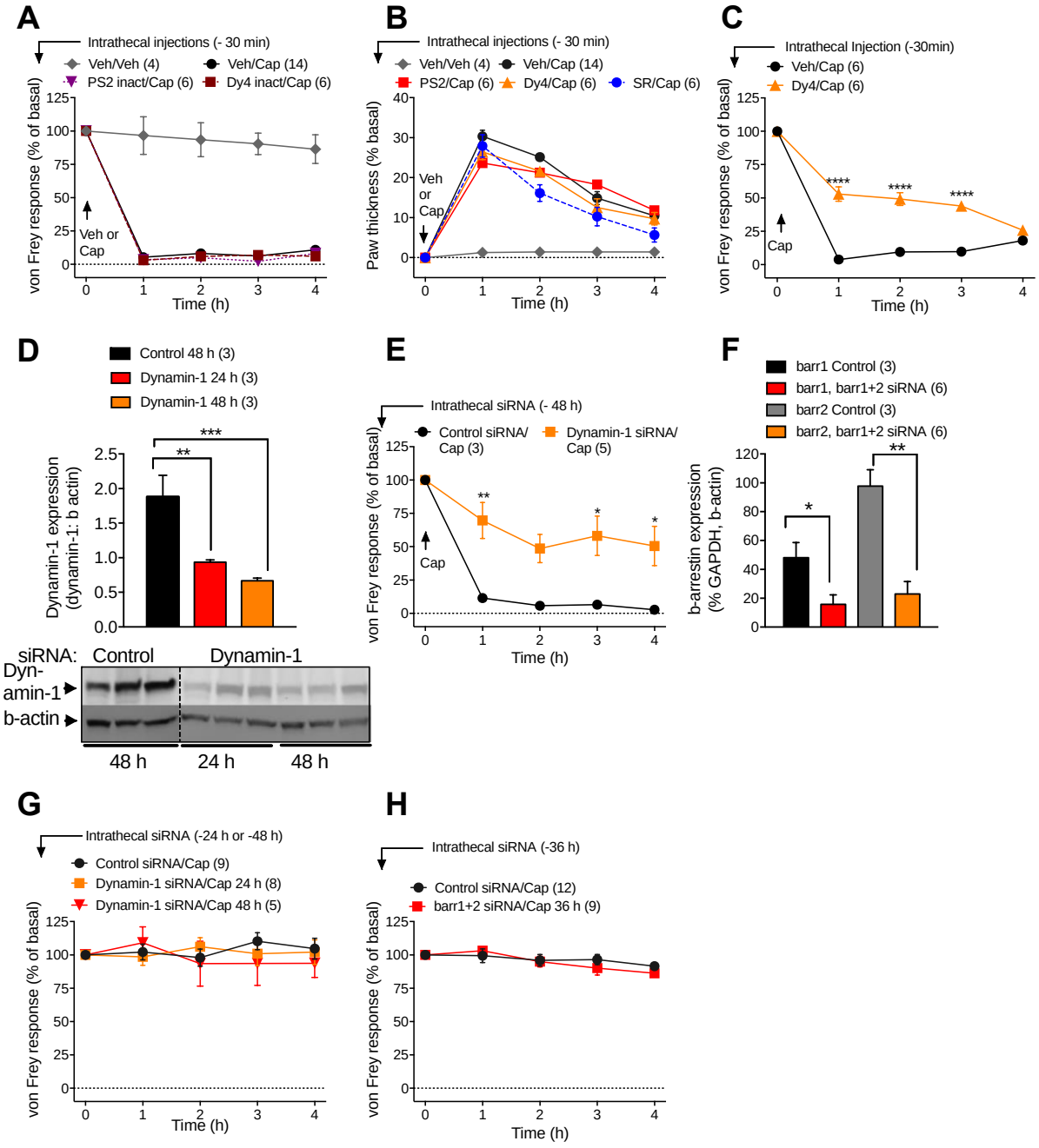

Fig. S4. Nociception and inflammation in vivo. A to **E.** von Frey withdrawal responses of capsaicin-injected paw after intrathecal injection of indicated inhibitors or inactive controls. **B.** Thickness of the capsaicin-injected paw after intrathecal injection of indicated inhibitors or inactive controls. **D** and **F.** Validation of siRNA knockdown of dynamin-1 (**D**, Western blot) and

βARR1+2 (**F,** qPCR) in the spinal cord. **G** and **H.** von Frey withdrawal responses of contralateral paw after siRNA knockdown of dynamin (**G**) or βARR1+2 (**H**). **P*<0.05, ***P*<0.01, ****P*<0.001, *****P*<0.0001 to control. All experiments were in mice except C, which was in rats. (*N*) animal number. ANOVA, Dunnett's test (A-C, E, G-H); Student's t test (D, F).

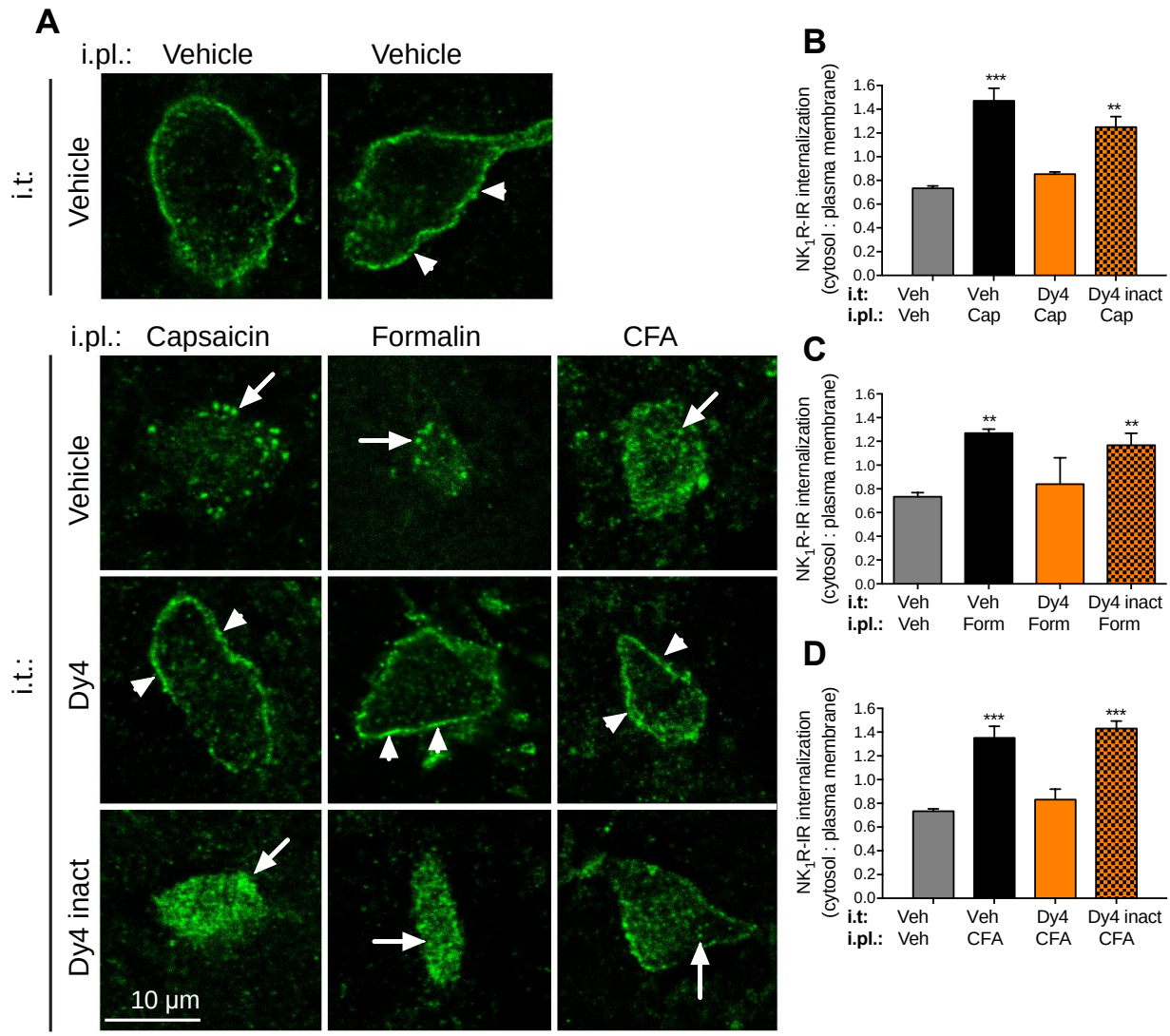

Fig. S5. NK$_1$R endocytosis in spinal neurons in vivo. A. NK$_1$R-IR localization in mouse spinal cord, 30 min after intraplantar (i.pl.) capsaicin, 90 min after intraplantar formalin, and 40 h after intraplantar CFA. Vehicle, Dy4, or Dy4 inact was injected intrathecally (i.t.) 30 min before intraplantar injection of capsaicin or formalin, or 36 h after intraplantar injection of CFA. Arrowheads, cell surface; arrows, endosomes. **B** to **D**. Cytosolic:plasma membrane NK$_1$R-IR in mouse spinal neurons. ***P*<0.01, ****P*<0.001 to vehicle. 18 neurons per condition (6 neurons from *N*=3 mice). Student's t test (B-D).

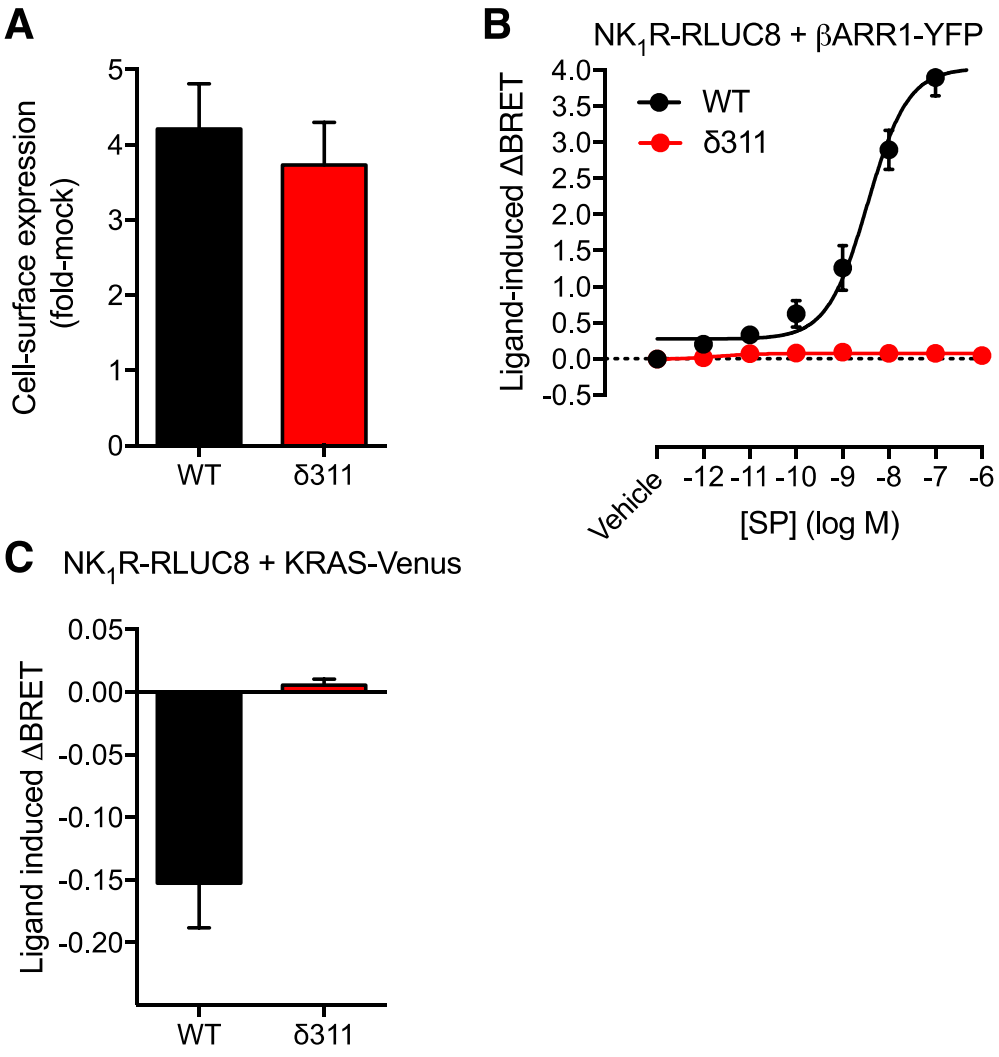

Fig. S6. NK$_1$Rδ311 expression and trafficking. A. Cell-surface ELISA of wild-type (WT) NK$_1$R and NK$_1$Rδ311 in HEK293 cells. **B** and **C.** SP-induced BRET between WT NK$_1$R-RLUC8 or NK$_1$Rδ311-RLUC8 and βARR1-YFP (**B**) or KRas-Venus (**C**). Triplicate observations, $N \geq 3$ experiments.

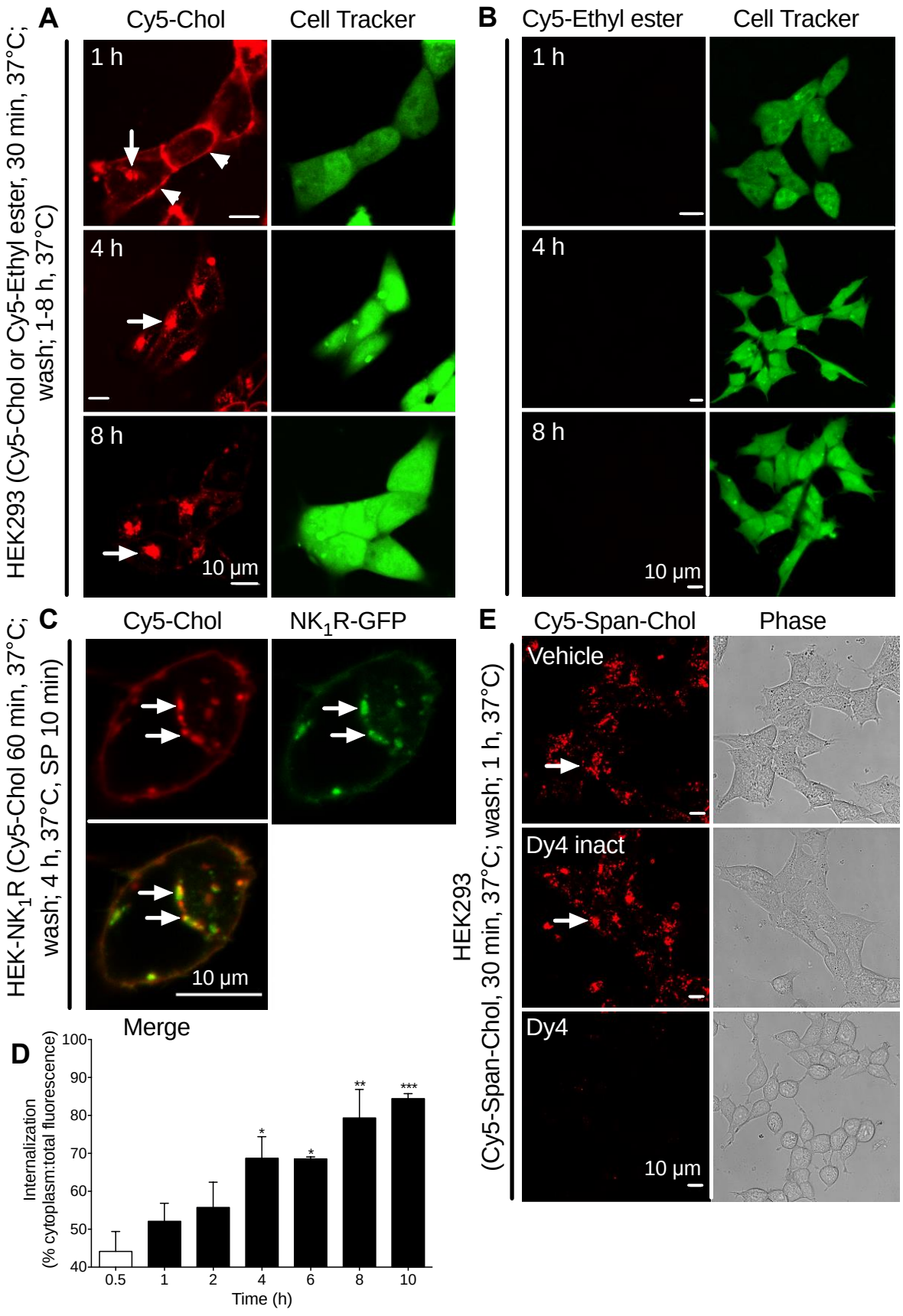
A
Cy5-Chol
Cell Tracker
1 h
4 h
8 h
10 µm
HEK293 (Cy5-Chol or Cy5-Ethyl ester, 30 min, 37°C; wash; 1-8 h, 37°C)
B
Cy5-Ethyl ester
Cell Tracker
1 h
4 h
8 h
10 µm
C
Cy5-Chol
NK1R-GFP
Merge
10 µm
HEK-NK1R (Cy5-Chol 60 min, 37°C; wash; 4 h, 37°C, SP 10 min)
D
Internalization (% cytoplasm:total fluorescence)
100
90
80
70
60
50
40
0.5
1
2
4
6
8
10
Time (h)
*
*
**
***
E
Cy5-Span-Chol
Phase
Vehicle
Dy4 inact
Dy4
10 µm
HEK293 (Cy5-Span-Chol, 30 min, 37°C; wash; 1 h, 37°C)

Fig. S7. Uptake of tripartite probes. A and **B.** Time course of Cy5-Chol (**A**) and Cy5-Ethyl ester (**B**) uptake into HEK293 cells. HEK293 cells were pulse-incubated with tripartite probes for 30 min, washed, and imaged at 1, 4, or 8 h after washing. Arrow heads, plasma membrane Cy5-Chol; arrows, internalized Cy5-Chol. **C.** Colocalization of Cy5-Chol and NK_1R-GFP. HEK-NK_1R cells were pulse-incubated with Cy5-Chol for 60 min, washed, and recovered for 4 h. Cells were then challenged with SP to induce NK_1R endocytosis. Arrows, colocalization of Cy5-Chol and NK_1R-GFP. **D.** Quantification of Cy5-Chol uptake. Cells were pulse-incubated with Cy5-Chol (as in A), washed, and recovered for 1-10 h. Cy5-Chol uptake was quantified. **P*<0.05, ***P*<0.001 to control. 6-9 cells, *N*=3 experiments. **E.** Effect of Dy4 and Dy4 inact on Cy5-Span-Chol uptake. Cells were pulse-incubated with Cy5-Span-Chol (as in A), washed, and recovered for 1 h. Arrows, Cy5-Chol in endosomes. ANOVA, Dunnett's test (D).

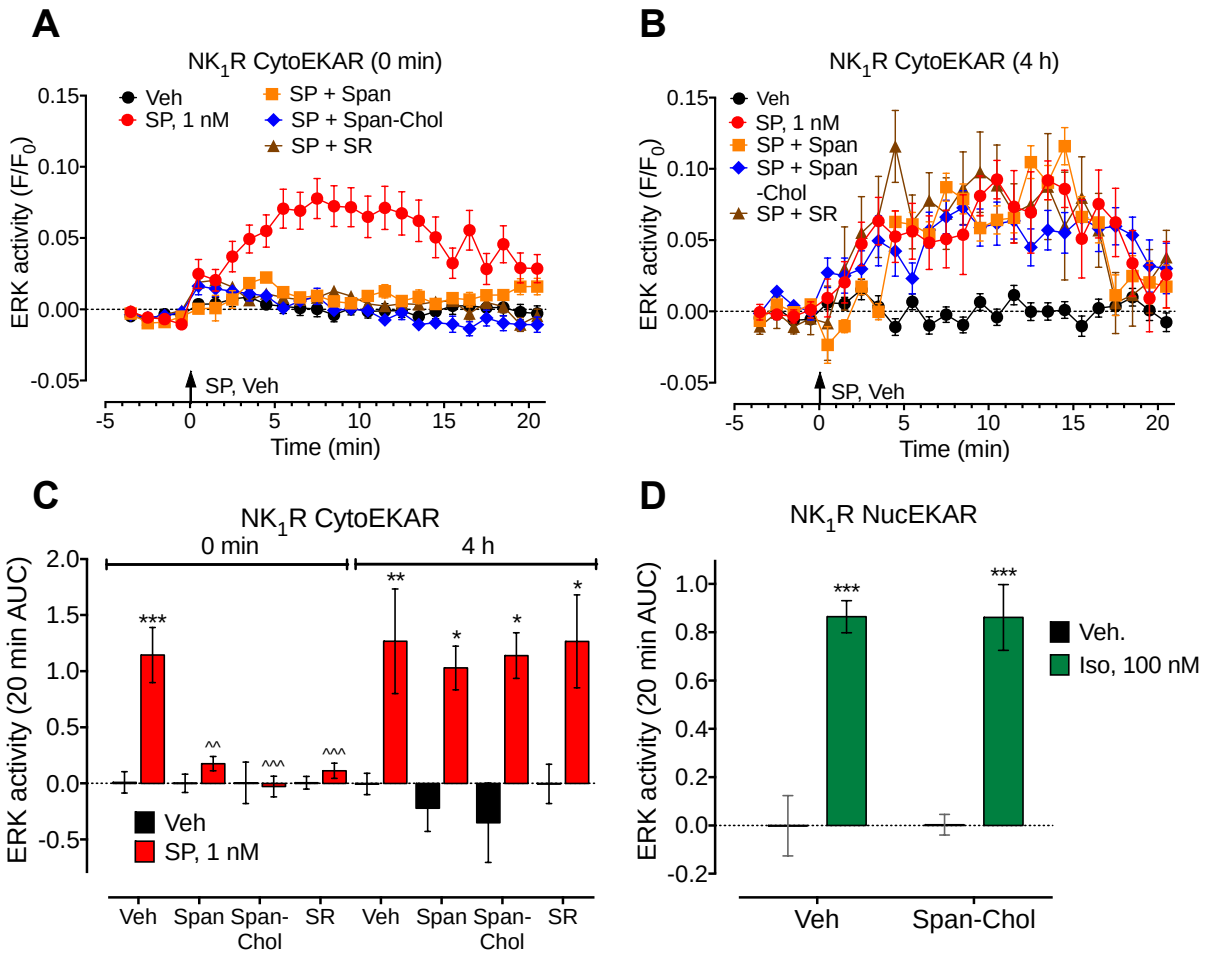

Fig. S8. Effects of NK$_1$R tripartite antagonists on ERK signaling. A to **C.** FRET assays for cytosolic ERK (CytoEKAR) immediately after (**A**, 0 min) or 4 h after (**B**, 4 h) 30 min preincubation with Span, Span-Chol, or SR140333 (SR). **C**. AUC for A and B. **D.** Effect of 4 h incubation with Span-Chol on the nuclear ERK response of endogenously expressed β_2AR. Iso, isoproterenol. **P*<0.05, ***P*<0.01, ****P*<0.001 SP to vehicle; ^^*P*<0.01, ^^^*P*<0.001 antagonist to control. 31-333 cells, 3 experiments. ANOVA, Tukey's test (C, D).

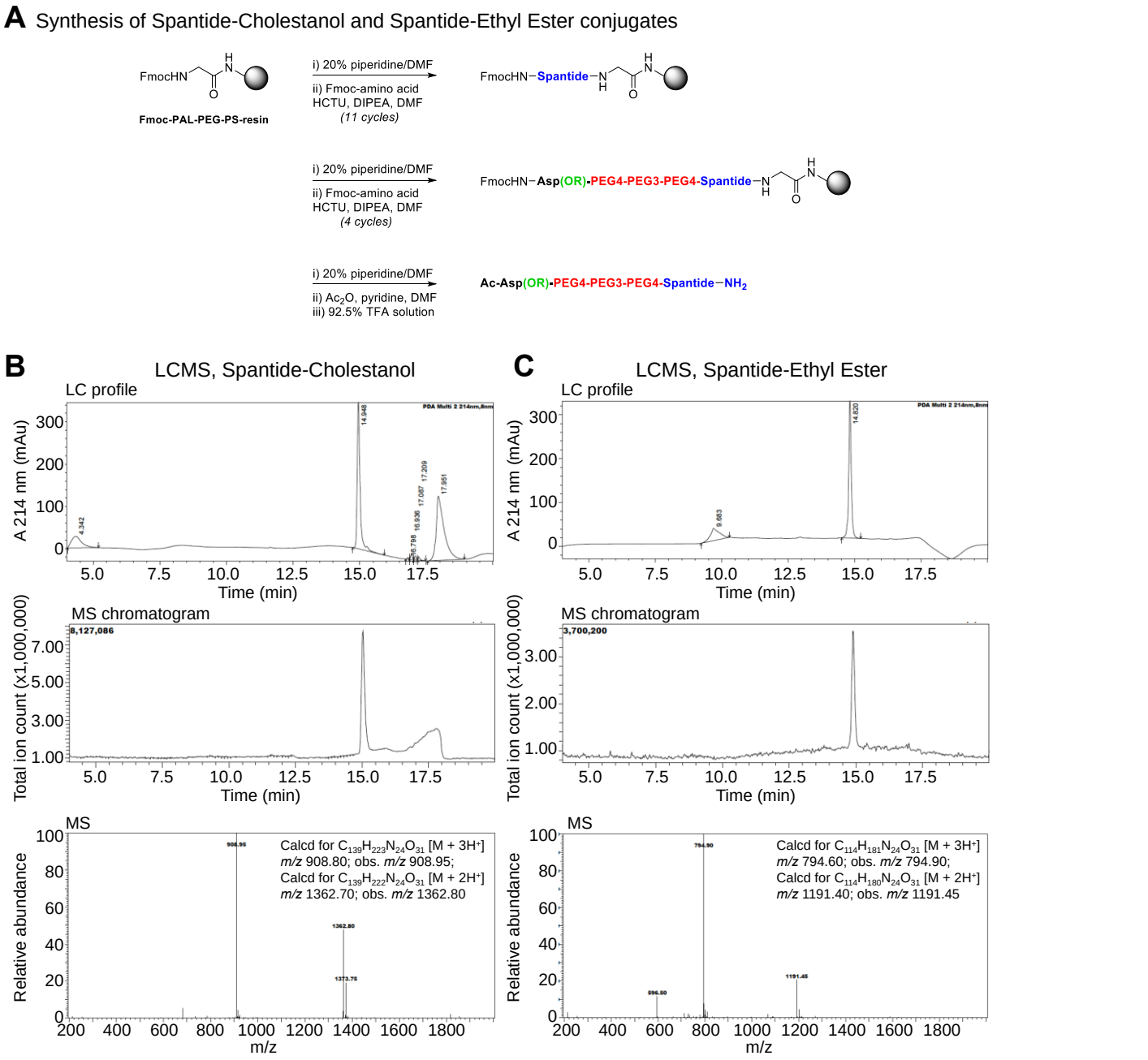

Fig. S9. Synthesis and analysis of Span-Chol and Span–ethyl ester. A. Synthesis of tripartite probes. **B.** LCMS analysis of Span-Chol. Peaks at t_R 4.34 and 17.95 min in the LC profile reflect changes in the baseline of the LC-MS gradient, as confirmed by injection of a blank solvent sample using the same method. **C.** LCMS analysis of Span-Ethyl ester. The peak at t_R 9.68 min

in the LC profile reflects changes in the baseline of the LC-MS gradient, as confirmed by injection of a blank solvent sample using the same method.

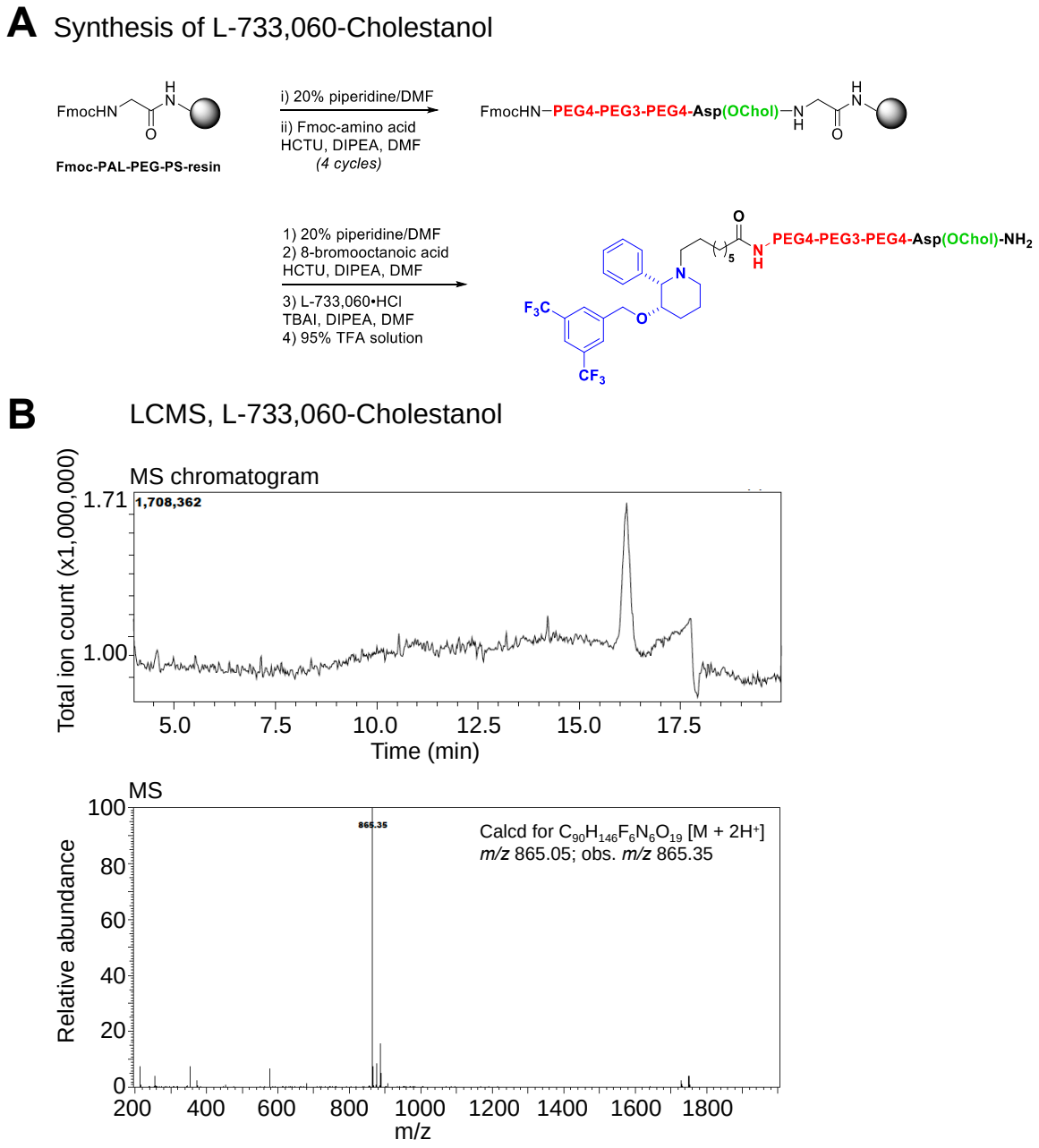

Fig. S10. Synthesis and analysis of L-733,060-Chol. A. Synthesis of tripartite probe. **B.** LCMS analysis. A UV spectrum for L-733,060-Chol could not be obtained because the absorbance of the construct was very low at both 214 and 254 nm, and the dominant peaks obtained were from the diluent buffer. The total ion trace (TIC) by MS is provided.

Table S1. Statistical analyses and cell replicates.

Figure	Test	Cell Number
Fig. 1 C, F, I, N	2-way ANOVA with Tukey's test	30-354 cells
Fig. 1 L	2-way ANOVA with Sidak's test	30-354 cells
Fig. 1 O	1-way ANOVA with Dunnett's test	Population based assay, N=3 experiments
Fig. 2 A-D	1-way ANOVA with Dunnett's test	Population based assay, $N \geq 3$ experiments
Fig. 2 F	1-way ANOVA with Sidak's test	60-66 cells
Fig. 2 G	2-way ANOVA with Sidak's test	35-67 cells
Fig. 2 H, I	2-way ANOVA with Tukey's test	35-67 cells
Fig. 3 B	2-way ANOVA with Tukey's test	6 neurons / animal / group
Fig. 3 D, G	2-way ANOVA with Sidak's test	6-7 neurons / animal / group
Fig. 3 E, H	1-way ANOVA with Dunn's test	6-7 neurons / animal / group
Fig. 4 C, D	Student's t-test unpaired	3 rats, ≥6 neurons or fields / rat
Fig. 4 E-M	1-way ANOVA with Dunnett's test	
Fig. 5 D	2-way ANOVA with Sidak's test	44-99 cells
Fig. 5 G	2-way ANOVA with Sidak's test	Population based assay, N=3 experiments
Fig. 5 H-J	1-way ANOVA with Dunnett's test	
Fig. 6 H	2-way ANOVA with Sidak's test	31-417 cells
Fig. 7 B	2-way ANOVA with Sidak's test	6-7 neurons / group
Fig. 7 C	1-way ANOVA with Dunn's test	6-7 neurons / group
Fig. 7 E-J	1-way ANOVA with Dunnett's test	

Supplementary Figures

Figure	Test	Cell Number
Fig. 1 E-H	1-way ANOVA with Dunnett's test	Population based assay, N=3 experiments
Fig. 2 C, E, G	2-way ANOVA with Tukey's test	16-354 cells
Fig. 2 J	2-way ANOVA with Sidak's test	16-354 cells
Fig. 4 A-C, E, G-H	1-way ANOVA with Dunnett's test	
Fig. 4 D, F	Student's T-test unpaired	
Fig. 5 B-D	Student's t-test unpaired	6 neurons / group
Fig. 7 D	1-way ANOVA with Dunnett's test	6-9 cells
Fig. 8 C, D	2-way ANOVA with Tukey's test	31-333 cells

Movie S1. Three-dimensional projections of NK_1R-IR in neurons in spinal cord slices incubated with Dy4 inact and vehicle. 3D projections of confocal images showing localization of NK_1R-IR in lamina I neurons in dorsal horn of rat spinal cord slices. Slices of spinal cord were preincubated with Dy4 inact (10 min), then incubated with vehicle (5 min), and fixed. Neurons from 3 animals are shown.

Movie S2. Three-dimensional projections of NK_1R-IR in neurons in spinal cord slices incubated with Dy4 inact and SP. 3D projections of confocal images showing localization of NK_1R-IR in lamina I neurons in dorsal horn of rat spinal cord slices. Slices of spinal cord were preincubated with Dy4 inact (10 min), then incubated with SP (1 µM, 5 min), and fixed. Neurons from 3 animals are shown.

Movie S3. Three-dimensional projections of NK_1R-IR in neurons in spinal cord slices incubated with Dy4 and vehicle. 3D projections of confocal images showing localization of NK_1R-IR in lamina I neurons in dorsal horn of rat spinal cord slices. Slices of spinal cord were preincubated with Dy4 (10 min), then incubated with vehicle (5 min), and fixed. Neurons from 3 animals are shown.

Movie S4. Three-dimensional projections of NK_1R-IR in neurons in spinal cord slices incubated with Dy4 and SP. 3D projections of confocal images showing localization of NK_1R-IR in lamina I neurons in dorsal horn of rat spinal cord slices. Slices of spinal cord were preincubated with Dy4 (10 min), then incubated with and SP (1 µM, 5 min), and fixed. Neurons from 3 animals are shown.

Movie S5. Three-dimensional projections of NK_1R-IR in neurons in spinal cord 10 min after intraplantar injection of vehicle. 3D projections of confocal images showing localization

of NK_1R-IR in lamina I neurons in dorsal horn of rat spinal cord. Tissues were collected 10 min after intraplantar injection of vehicle. Neurons from 3 animals are shown.

Movie S6. Three-dimensional projections of NK_1R-IR in neurons in spinal cord 10 min after intraplantar injection of capsaicin. 3D projections of confocal images showing localization of NK_1R-IR in lamina I neurons in dorsal horn of rat spinal cord. Tissues were collected 10 min after intraplantar injection of capsaicin. Neurons from 3 animals are shown.

Movie S7. Three-dimensional projections of NK_1R-IR in neurons in spinal cord 10 min after intraplantar injection of capsaicin, with Dy4 injected before capsaicin. 3D projections of confocal images showing localization of NK_1R-IR in lamina I neurons in dorsal horn of rat spinal cord. Tissues were collected 10 min after intraplantar injection of capsaicin. Dy4 was administered intrathecally 30 min before intraplantar capsaicin. Neurons from 3 animals are shown.

Movie S8. Three-dimensional projections of NK_1R-IR in neurons in spinal cord 10 min after intraplantar injection of capsaicin, with Dy4 inact injected before capsaicin. 3D projections of confocal images showing localization of NK_1R-IR in lamina I neurons in dorsal horn of rat spinal cord. Tissues were collected 10 min after intraplantar injection of capsaicin. Dy4 inact was administered intrathecally 30 min before intraplantar capsaicin. Neurons from 3 animals are shown.

Movie S9. Three-dimensional projections of NK_1R-IR in neurons in spinal cord 10 min after intraplantar injection of capsaicin, with PS2 injected before capsaicin. 3D projections of confocal images showing localization of NK_1R-IR in lamina I neurons in dorsal horn of rat spinal cord. Tissues were collected 10 min after intraplantar injection of capsaicin. PS2 was

administered intrathecally 30 min before intraplantar capsaicin. Neurons from 3 animals are shown.

Movie S10. Three-dimensional projections of NK_1R-IR in neurons in spinal cord 10 min after intraplantar injection of capsaicin, with PS2 inact injected before capsaicin. 3D projections of confocal images showing localization of NK_1R-IR in lamina I neurons in dorsal horn of rat spinal cord. Tissues were collected 10 min after intraplantar injection of capsaicin. PS2 inact was administered intrathecally 30 min before intraplantar capsaicin. Neurons from 3 animals are shown.

Movie S11. Plasma membrane incorporation and endocytosis of Cy5-cholestanol by HEK293 cells. Time lapse images showing plasma membrane incorporation and endocytosis of Cy5-cholestanol by HEK293 cells at 37°C. Cy5-cholestanol was added at 0 min.

Movie S12. Lack of uptake of Cy5–ethyl ester by HEK293 cells. Time lapse images showing lack of uptake of Cy5-ethyl ester by HEK293 cells at 37°C. Cy5-ethyl ester was added at 0 min.

Movie S13. Time lapse images showing FRET between SNAP-549-NK_1R and Cy5-Chol. Time lapse images showing FRET between SNAP-549-NK_1R and Cy5-cholestanol. SNAP-549-NK_1R was internalized by SP (10 nM, 30 min), and Cy5-cholestanol was added at 0 min. Scale, 10 μm.

Movie S14. Animation showing SP-induced assembly of endosomal signaling platform for pain transmission.